Supporting Information

Luo et al. 10.1073/pnas.1714760115

SI Materials and Methods

Study Approval. All of the animal experiments were performed in accordance with recommendations in the Guide for the Care and Use of Laboratory Animals of Kunming Institute of Zoology, Chinese Academy of Sciences. Experimental protocols using animals in this study were approved by the Institutional Animal Care and Use Committees at Kunming Institute of Zoology, Chinese Academy of Sciences (approval ID: SMKXLLWYH20120520-01).

Video Recording of Centipede's Bite. The body weights of the centipede (*Scolopendra subspinipes mutilans*) and Kunming mice (both sexes) were weighed, respectively. The mice were put into a 2-L conical flask to adapt to the environment. The centipede was delivered into the conical flask after the mice were stabilized. Thereafter, the time taken for the mice to be subdued was recorded.

Mice Lethality Assay. The LD_{50} of toxin in Kunming mice (both sexes; aged 6–8 wk; weight: 20–25 g) was defined as the dose of SsTx or crude venom that causes the death of 50% of challenged populations within 24 h. These mice were housed at a constant temperature of 24 °C under controlled conditions of 12-h light/dark cycles and provided with free access to laboratory-standard food and water. SsTx or crude venom was injected i.v., s.c., and into the intracranial hippocampus in different test groups, respectively. Three or four mice were used for each test group (n = 3). The mortality of mice was recorded for 24 h after venom injection.

Venom Collection, SsTx Purification, and Protein Sequencing. A total of 1,000 adult *S. subspinipes mutilans* (both sexes) were purchased from Anhui Province, China. As previously reported (1, 2), a 3-V alternating current was used to manually stimulate the venom gland to collect the crude venom. SsTx was purified from the raw venom using a combination of a Sephadex G-50 gel filtration column, FPLC, and RP-HPLC. The purity and molecular weight of toxin were analyzed using a MALDI-TOF-MS (Bruker Daltonik GmBH). The toxin with purity >99% was collected and stored at −20 °C until further use. Primary amino acid sequences were obtained by automated Edman degradation using a Shimadzu protein sequencer (PPSQ-31A; Shimadzu). The crude venom used in coronary artery assays consisted of protein peaks I-V from G-50 gel filtration column and all protein fractions of G-50 peak VI from RP-HPLC. The only difference between crude venom and CV-Sf was that SsTx was separated from the protein fractions of G-50 peak VI. Briefly, the SsTx was isolated from the crude venom using a combination of a Sephadex G-50 gel filtration column, FPLC, and RP-HPLC. The rest of the venom fractions were pooled and lyophilized for the reconstitution of CV-Sf.

Determination of Disulfide Bridge Connections. SsTx (0.1 mg) was partially reduced in 10 μL of citrate buffer (1 M, pH 3.0) containing 6 M guanidine-HCl and 0.05 M Tris (2-carboxyethyl) phosphine (TCEP) for 8 min at 37 °C. The partially reduced sample was fractionated by C_{18} RP-HPLC using a linear acetonitrile gradient (0–50% over 100 min). The second fraction with one pair of free thiols was collected and determined using MALDI-TOF-MS. Reduced SsTx with two free thiols was lyophilized and alkylated with iodoacetamide (0.5 M, pH 6.0). Alkylated peptides were purified, desalted using C_{18} RP-HPLC, and detected by MALDI-TOF/TOF-MS to confirm their homogeneity. The alkylated peptide was then digested by trypsin at 37 °C for 2 h with a final trypsin:peptide ratio of 1:50 (wt:wt). The digested products mixed with α-cyano-4-hydroxycinnamic acid were detected by MALDI-TOF/TOF-MS to screen for the disulfide-linked peptide using a previously reported equation (3). Putatively disulfide-linked peptides were subjected to laser ionization fragmentation technology (LIFT)-TOF/TOF-MS to confirm the disulfide linkage pattern. The results were analyzed by Bruker software (SequenceEditor and Biotool 3.2).

NMR Data Acquisition and Structure Determination. The native SsTx sample for NMR measurement contained 5 mmol/L SsTx in 500 μL of 90% PBS/10% D_2O at pH 6.5. All NMR experiments were carried out on a 700 MHz Varian spectrometer equipped with three RF channels. The 2D TOCSY spectrum was acquired with a mixing time of 75 ms. NOESY spectra were acquired with mixing times of 100, 200, and 300 ms. Both the Watergate approach and the presaturation scheme were employed for water suppression. All spectra were recorded with 400 t1 increments and 2,048 complex data points. Signals were averaged over 32 transients. All NMR data were processed and analyzed using the NMRPipe/NMRDraw software and the Sparky program (4, 5). Linear prediction in the t1 dimension was used before the Fourier transformation. ^1H resonance assignments were performed using TOCSY, NOESY, and DQF-COSY spectra for identification of the scalar coupled spin systems and the sequential connectivity. Structure calculations were performed according to the standard ARIA/CNS protocol (6, 7). A family of 200 structures was calculated according to the simulated annealing protocol, and the 20 lowest-energy structures were finally selected. The rmsd values for the backbone atoms of secondary structural regions were 0.690 Å, calculated by the program MOLMOL. Ramachandran plot analysis was performed using the PROCHECK program. The electrostatic potential graph was displayed by the software Discovery Studio 3.1.

Peptides Synthesis, Refolding, and Purification. An automatic peptide synthesizer (PerSeptive Biosystems) with an Fmoc/tert-butyl strategy and HOBt/TBTU/NMM coupling method to synthesize linear SsTx or point mutants was used. Crude peptidic products were purified by RP-HPLC. Once the purity of linear SsTx or point mutants was determined to be >95% by MALDI-TOF-MS and HPLC, the peak was pooled and lyophilized. The linear reduced peptide was dissolved in 0.1 M Tris·HCl and 0.1 M sodium chloride buffer (pH 8.0) at a final concentration of 30 μM glutathione containing 5 mM reduced glutathione and 0.5 mM oxidized glutathione at 28 °C for 24 h. Oxidized and folded peptides were fractionated by analytical C_{18} RP-HPLC using a linear acetonitrile gradient, and the purity was detected by MALDI-TOF-MS.

Circular Dichroism Spectroscopy. Circular dichroism (CD) spectra of SsTx or point mutants (20 μM in ultrapure water, pH 7.2) were acquired at 20 °C under constant N2 flush using a Jasco J-810 spectrophotometer. The secondary and tertiary structures of purified SsTx and its mutants were determined by obtaining CD spectra at far-UV (250–190 nm) and near-UV (350–250 nm), respectively. Far-UV CD spectra were obtained in 0.1-mm path-length circular cuvettes, while near-UV spectra were sampled in 10-mm path-length standard quartz cuvettes. All data were collected using a step resolution of 1 nm, a scan speed of 50 nm/min, and a response time of 1 s. Measurements were performed over 10 accumulations to reduce the signal-to-noise ratio and were

baseline-corrected against the storage buffer. Protein concentrations were ~1.0 mg/mL; CD measurements were converted to units of molar ellipticity ([θ]). All corrections and processing were undertaken using the Jasco Standard Analysis Program.

Cell Culture, Mutagenesis, Transient Transfection, and Electrophysiology. HEK293T cells were cultured as previously reported (3). All KCNQ point mutations were constructed using the QuikChange II XL site-directed mutagenesis kit (Agilent Technologies) following the manufacturer's instructions. These point mutations were sequenced to confirm that appropriate constructs were made. HEK293T cells were cultured and transiently transfected using Lipofectamine 2000 (Invitrogen) as previously described (3). Macroscopic currents were recorded using a HEKA EPC10 amplifier with the PatchMaster software (HEKA) (2). During whole-cell recording, voltage errors were minimized using 80% series resistance compensation, and the capacitance artifact was canceled using the computer-controlled circuitry of the patch-clamp amplifier. Patch pipettes were pulled from borosilicate glass and fire-polished to a resistance of 3–6 MΩ. All recordings were performed at room temperature. To evoke KCNQ currents, a holding potential of −80 mV was used, from which a testing pulse to 0 mV was applied. The wash-in and wash-out currents were recorded with a holding potential of −80 mV for 200 ms and a testing potential of 0 mV for 5,000 ms. The dose–response relationships and the wash-in and wash-out rates were determined using a solution exchanger, RSC-200, with eight separate tubes to deliver different concentrations of SsTx. The tube number sent by the solution exchanger was fed into an analog input port of the EPC10 patch-clamp amplifier, and current was recorded simultaneously. The stable current amplitude at different concentrations was recorded. For KCNQ channel recording, the pipette solution contained (in mM): 160 KCl, 5 $MgCl_2$, and 5 Hepes (pH 7.2). Bath solution contained (in mM): 160 NaCl, 2.5 KCl, 2 $CaCl_2$, 1 $MgCl_2$, 10 glucose, and 10 Hepes (pH 7.4). For TRP channel recording, the pipette solution and bath solution contained (in mM): 130 NaCl, 3 Hepes, and 0.2 EDTA (pH 7.2). For voltage-gated sodium channels, pipette solution contained (in mM): 135 CsF, 10 NaCl, and 5 Hepes at pH 7.0; and external bath composition was (in mM): 30 NaCl, 5 CsCl, 25 D-glucose, 1 $MgCl_2$, 1.8 $CaCl_2$, 5 Hepes, 20 triethanolamine-chlorine, and 70 tetramethylammonium chloride at pH 7.4. For voltage-gated calcium channels, external recording solution contained (in mM): 130 choline chloride, 0.0025 TTX, 25 TEA-Cl, 3 KCl, 5 $BaCl_2$, 0.6 $MgCl_2$, 1 $NaHCO_3$, 10 Hepes, 4 glucose, adjusted pH to 7.4 with NaOH and pipette solution containing (in mM): 140 CsCl, 10 EGTA, 0.1 $CaCl_2$, 2 $MgCl_2$, 10 Hepes, 2 ATP, adjusted pH to 7.2 with Tris. For voltage-gated potassium channels, the internal solution contained (in mM): 140 KCl, 10 EGTA, 10 Hepes, and 4 MgATP, adjusted pH to 7.2 with KOH; and the bath solution contained (in mM): 135 NaCl, 5.4 KCl, 1 $MgCl_2$, 0.33 NaH_2PO_4, 10 glucose, and 10 Hepes, adjusted pH to 7.4 with NaOH. For BK_{Ca} channel recording, the internal solution contained (in mM): 160 $MeSO_3K$, 10 Hepes, and 5 EGTA with added Ca^{2+} to make 1 μM free Ca^{2+}; and the bath solution contained (in mM): 160 MeSO3K, 10 Hepes, and 2 MgCl2, adjusted to pH 7.0 with MeSO3H.

Action Potential Recordings from Human Pluripotent Stem Cell-Derived Cardiomyocytes. Differentiation of human pluripotent stem cell-derived cardiomyocytes (hiPSC-CMs) from embryoid bodies was performed according to our previous report by using standard 3D differentiation protocols (8). Human embryonic stem cell (H9)-derived cardiomyocytes (H9-CMs) were enzymatically and mechanically disrupted to produce single cells, which were seeded on Matrigel-coated glass coverslips. Action potentials were recorded from H9-CMs paced at 1 Hz using an EPC-10 patch clamp amplifier (HEKA). Continuous extracellular solution perfusion was achieved using a rapid solution exchanger (RSC-200; Bio-logic). Data were acquired using PatchMaster software (HEKA) and digitized at 1 kHz. Data analysis was done using Igor Pro (Wavemetrics) and Prism (GraphPad). A TC-344B heating system (Warner) was used to maintain the temperature at 35.5–37 °C. Tyrode solution was used as the bath solution containing (in mM):150 NaCl, 5.4 KCl, 1 $MgCl_2$, 15 glucose, 1.8 $CaCl_2$,1 Na-pyruvate, and 15 Hepes (pH 7.4 with NaOH at 25 °C). The pipette solution contained (in mM):150 KCl, 5 NaCl, 2 $CaCl_2$, 10 Hepes, 5 Mg-ATP, and 5 EGTA (pH 7.2 with KOH at 25 °C).

Thoracic Aorta Isolation and Vascular Reactivity. Six Sprague-Dawley rats (aged 7–9 wk, 200–250 g, female) were adopted for the vascular contractility study. The thoracic aorta was quickly isolated and placed in Krebs solution containing (in mM): 120 NaCl, 1.2 $CaCl_2$, 1.2 $MgSO_4$, 5 KCl, 1 NaH_2PO_4, 25 $NaHCO_3$, 12 glucose, and 10 Hepes (pH 7.4, 37 °C), aerated with 95% O_2 and 5% CO_2. The aorta segments were cut into rings (3-mm long) and mounted on two stainless-steel wires passing through the vessel lumen. Arterial isometric tension recording was carried out with a myograph system (Techman) connected to a computer. Each vessel device was placed individually in 10 mL tissue bath.

Bronchial Ring Isolation and Contraction Bioassay. Six Sprague-Dawley rats (aged 7–9 wk, 200–250 g, female) were adopted for the bronchial ring contractility study. The bronchus was quickly isolated and placed in Krebs solution containing (in mM): 118.07 NaCl, 2.52 $CaCl_2$, 1.16 $MgSO_4$, 4.69 KCl, 1.01 NaH_2PO_4, 25 $NaHCO_3$, 11.1 glucose, and 10 Hepes (pH 7.2–7.4, 37 °C), aerated with 95% O_2 and 5% CO_2. Bronchial rings of ~2.5 mm in length were cut and attached to mounting support pins that were connected to force transducers, and changes in their force were recorded with a HV-4 in vitro tissue temperature perfusion system connected to a computer. Each vessel device was placed individually in 10 mL tissue bath. The bronchial rings were kept in oxygenated Krebs buffer (95% O_2 + 5% CO_2) at 37 °C. After a 20-min equilibrium, a 0.5-g stretch was applied to the rings three times with a 5-min interval. Testing samples were then used to stimulate the rings.

Measurement of Respiratory Frequency and Amplitude in Rats. Sprague-Dawley rats (aged 7–9 wk, 200–250 g, female, $n = 3$) were anesthetized by i.p. injection of 1% pentobarbital sodium (30 mg/kg), and limbs were fixed on the operating table for easy operation. The rats' neck hair was removed and disinfected with iodine. The fascia and the anterior cervical muscle group were separated, and the trachea was cut into a T-shaped incision. A clean tube matching with the diameter of the trachea was gently inserted, and the silk ligation fixation was used to prevent shedding. The HX200 respiratory flow sensor and the three-channel electrode were connected to the BL-420F biological function experimental system for measurement of the respiratory frequency and amplitude.

Measurement of Hemodynamic Responses. A total of three healthy male macaques (*Macaca mulatta*), aged 2–3 y and weighing 3.5–4.5 kg, were randomly selected for experiments. Macaques were fixed on a table in the prone position. Systolic blood pressure (SBP), diastolic blood pressure (DBP), and heart rates were recorded in 3-min segments using automated devices (YE660D; Yuwell) under anesthesia (i.m. injection of 20 mg/kg ketamine hydrochloride). After SBP and DBP were stable, 1 mg/kg atropine was applied for the antagonism of vasospasm.

The hemodynamic responses of adult C57BL/6J mice were recorded. Briefly, the mice were placed in a mouse net, and the mice tails were fixed. Then, the mice were placed in a 38 °C insulation barrel to warm up for 15 min to stabilize the local blood vessels and a pressure sensor was placed on the mouse tail. The measurement of blood pressure began after the mice had calmed down. Each mouse was measured six times, and the

average value of the results was taken as the final result and the SBP and DBP were recorded. SsTx (0.5 mg/kg, $n = 10$) or saline ($n = 10$) in the same volume were i.v. injected. Five minutes postinjection, SBP and DBP were recorded by using a Softron intelligent noninvasive blood pressure meter (BP-98A; Softron Biotechnology).

Surface ECG Measurements. Healthy male macaques (*M. mulatta*, $n = 3$, aged 2–3 y, and weighing 3.5–4.5 kg) were randomly selected for experiments. The animals were placed in a supine position, and three limbs (two front paws, left leg) were attached to gel-covered silver wire loops. A three-lead surface ECG signal was recorded. The signals were preamplified and displayed on a computer (ECG parameters gain, 1 mV. high-pass filtering, 0.1 s. low-pass filtering, 100 Hz). ECG data were acquired and analyzed by using AcqKnowledge Software (BIOPAC Systems, Inc.).

Slice Preparation and Electrophysiological Recording. Coronal brain slices containing the substantia nigra pars compacta (SNc) were prepared from postnatal day 14–21 Sprague-Dawley rats of either sex. Animals were anesthetized with pentobarbital sodium and decapitated. Their brains were quickly removed and placed into an ice-cold sucrose slicing solution containing the following (in mM): 250 glycerol, 2.5 KCl, 2 $MgCl_2$, 2 $CaCl_2$, 1.2 NaH_2PO_4, 10 Hepes, 21 $NaHCO_3$, and 5 glucose, bubbled with 95/5% O_2/CO_2. Slices were cut (300-μM thick) and incubated for 30 min at 24 °C in artificial CSF (ASCF) consisting of the following (in mM): 125 NaCl, 25 $NaHCO_3$, 1.25 NaH_2PO_4, 3.5 KCl, 1 $MgCl_2$, 2 $CaCl_2$, and 10 glucose, bubbled with 95/5% O_2/CO_2. Slices were stored at room temperature until use.

Slices were placed into a heated recording chamber (24 ± 1 °C) and continuously perfused with ACSF at a rate of 3 mL/min until the recording began. The soma of CA1 pyramidal neurons in the SNc were visualized using a CCD camera (Hamamatsu) on an Olympus microscope (BX51). Recordings were made with a Multiclamp 700B amplifier (Molecular Devices) using borosilicate patch electrodes (1–4 MΩ) wrapped with Parafilm to reduce pipette capacitance. Pipette series resistance (typically 2–5 MΩ) was compensated by 70% during voltage-clamp experiments and was checked frequently throughout the experiment. Current and voltage signals were filtered at 10 kHz and sampled at 20 μs using a Digidata 1440A data acquisition interface (Molecular Devices) and pClamp 10 software (Molecular Devices). The internal solution contained the following (in mM):122 K methanesulfonate, 9 NaCl, 1.8 $MgCl_2$, 4 Mg-ATP, 0.3 Na-GTP, 14 phosphocreatine, 0.45 EGTA, 0.1 $CaCl_2$, and 10 Hepes, pH adjusted to pH 7.35 with KOH. Experiments were done at 24 ± 1 °C.

Stereotaxic Surgery and Microinjections. Adult C57BL/6J mice weighing 23–25 g (male, aged 6–8 wk) were sedated via i.p. injection of pentobarbital sodium (0.3 mL/100 g body weight) and placed in a Stoelting stereotaxic instrument. The mouse heads were fixed using a Stoelting stereotaxic instrument and a 0.5-mm incision on the mouse head was made with a stainless-steel blade along the head midline. Stereotaxic coordinates for the mouse skull regions were transverse 1.6 mm and longitudinal 1.4 mm. The hippocampus was infused by means of an internal cannula, which terminated 1.75 mm below the skull, and connected by polyethylene tubing to a 1-μL Hamilton syringe. SsTx was injected by a Stoelting stereotaxic intracranial dosing pump with a speed of 1 μL/min. The inner cannula was left in place for an additional 60 s to allow diffusion of the solution and to reduce the possibility of reflux. The mouse hippocampus that was injected was immediately removed from the brain and preserved in liquid nitrogen for ELISA test.

Acetylcholine Quantification. Acetylcholine concentration was quantified following the instructions of BioVision's Choline/Acetylcholine Quantification Kit (BioVision, Inc.). Briefly, tissue was lysed in Choline Assay Buffer by homogenization on ice, and then centrifuged to remove debris. Acetylcholinesterase was omitted to detect free choline only, and total and free choline were individually measured. OD at 570 nm was monitored for the colorimetric assay, and the OD readings were converted to choline amount using a standard curve. The choline concentrations of the test samples were then calculated.

Tissue Necrosis Assay. Male Kunming mice (aged 6–8 wk, $n = 6$) were anesthetized using 1% pentobarbital sodium (0.1 mL/20 g body weight). Dorsal hairs were removed by an electric clipper, and the dorsal skin was cleansed with Betadine. Ten microliters of saline and SsTx (10 μM dissolved in saline) were injected under the skin on the back of each mouse (saline on the left side, SsTx on the right side). The phenotype of skin tissues was monitored after sample injection. Skin tissues for histological examination were removed and fixed in 4% formalin and embedded in paraffin. Sections (thickness = 3 μm) of the dorsal skin were stained by hemotoxylin and eosin.

Construction of KCNQ4 Channel Model. A partial model of KCNQ4 subunit (NP_004691) was constructed from R95 to K333 by homology modeling (MODELER) based on our previous KCNQ1 model (9). A tetrameric KCNQ4 channel was then assembled by applying a fourfold symmetry. The KCNQ4 channel model was inserted into implicit membranes and energy minimized by 100 ps of standard molecular dynamics process with the Discovery Studio 3.1 suite.

Docking and Refinement of SsTx/KCNQ4 Complexes. One conformation of SsTx was extracted from the NMR-determined ensemble and docked into the KCNQ4 tetramers by the standard peptide-peptide docking protocol of the Discovery Studio. During the docking process, common parameters were used to obtain more accurate results and ZRank scored top 2,000 poses with an rmsd cutoff of 10.0 Å. The docking protocol reported 54,000 docked poses; among them, 2,962 poses passed filters and almost 94 clusters were produced out of 2,000 poses by the docking process. The largest cluster contained 142 poses. With the experimentally known interaction pair of D266 (KCNQ4)-K13 (SsTx) as a constraint along with common parameters, the peptide was docked to the local area of KCNQ4, and another key interaction pair, D288 (KCNQ4)-R12 (SsTx), was determined.

The docked complex of SsTx/KCNQ4 was further optimized by molecular dynamic (MD) simulations. The SsTx/KCNQ4 complex was inserted into an implicit membrane and Charmm Force Field was used to parameterize the atom types of the complex. MD simulation of the ensemble class was conducted under constant number of particles, pressure, and temperature (300 K) with a time step of 2 fs. The Discovery Studio Suite was used for simulation and visualization including the parameterization of the whole complex ensemble.

Data Analysis. The results are expressed as means ± SEMs. Student's t test was applied to examine statistical significance. Statistical significance was accepted at a level of $P < 0.05$. Data from whole-cell recordings were analyzed by Igor Pro (WaveMatrix).

G-V curves were fitted to a single Boltzmann function.

$$\frac{G}{G_{max}} = \frac{1}{1 + e^{-\frac{zF}{RT}(V - V_{half})}}$$

Where G/G_{max} is the normalized conductance, z is the equivalent gating charge, V_{half} is the half-activation voltage, F is the Faraday's constant, R is the gas constant, and T is the temperature in Kelvin.

IC_{50} values were derived from fitting a Hill equation to the concentration–response relationship. Changes in IC_{50} by point mutation may be caused by perturbation of ligand binding.

$$\frac{I_x}{I_{max}} = 1 - \frac{[X]^n}{IC_{50}^n + [X]^n}$$

Where I_x represents the difference between the steady-state KCNQ current and the leaking current in the presence of concentration [x], I_{max} represents the difference between the maximal current amplitude and the leaking current. IC_{50} is the concentration for the half-maximal effect. The leaking current is the current level in the presence of saturated linopirdine. The currents were normalized by I_{max} and the inhibitory currents were normalized by the inhibitory currents in the presence of saturated linopirdine unless otherwise stated.

To perform double-mutant cycle analysis, IC_{50} values of the four channel-ligand combinations (WT channel, WT toxin: IC_{50}_1; mutant channel, WT toxin: IC_{50}_2; WT channel, mutant toxin: IC_{50}_3; mutant channel, mutant toxin: IC_{50}_4) were determined separately. The interaction between residues was determined as LnΩ. LnΩ was calculated as value (10) without units of energy, because multiple toxins act with positive cooperativity to inhibit the channels. So that LnΩ in this study should not be compared directly to those in the cited literature.

$$\ln \Omega = \ln\left(\frac{IC50\_1 \cdot IC50\_4}{IC50\_2 \cdot IC50\_3}\right)$$

1. Yang S, et al. (2012) Chemical punch packed in venoms makes centipedes excellent predators. *Mol Cell Proteomics* 11:640–650.
2. Yang S, et al. (2013) Discovery of a selective NaV1.7 inhibitor from centipede venom with analgesic efficacy exceeding morphine in rodent pain models. *Proc Natl Acad Sci USA* 110:17534–17539.
3. Yang S, et al. (2015) A pain-inducing centipede toxin targets the heat activation machinery of nociceptor TRPV1. *Nat Commun* 6:8297.
4. Delaglio F, et al. (1995) NMRPipe: A multidimensional spectral processing system based on UNIX pipes. *J Biomol NMR* 6:277–293.
5. Nilges M, Macias MJ, O'Donoghue SI, Oschkinat H (1997) Automated NOESY interpretation with ambiguous distance restraints: The refined NMR solution structure of the Pleckstrin homology domain from beta-spectrin. *J Mol Biol* 269: 408–422.
6. Brünger AT, et al. (1998) Crystallography & NMR system: A new software suite for macromolecular structure determination. *Acta Crystallogr D Biol Crystallogr* 54: 905–921.
7. Brünger AT (2007) Version 1.2 of the crystallography and NMR system. *Nat Protoc* 2: 2728–2733.
8. Navarrete EG, et al. (2013) Screening drug-induced arrhythmia [corrected] using human induced pluripotent stem cell-derived cardiomyocytes and low-impedance microelectrode arrays. *Circulation* 128(11, Suppl 1):S3–S13, and erratum (2014) 129:e452.
9. Li P, et al. (2014) Differential modulations of KCNQ1 by auxiliary proteins KCNE1 and KCNE2. *Sci Rep* 4:4973.
10. Schreiber G, Fersht AR (1995) Energetics of protein-protein interactions: Analysis of the barnase-barstar interface by single mutations and double mutant cycles. *J Mol Biol* 248:478–486.

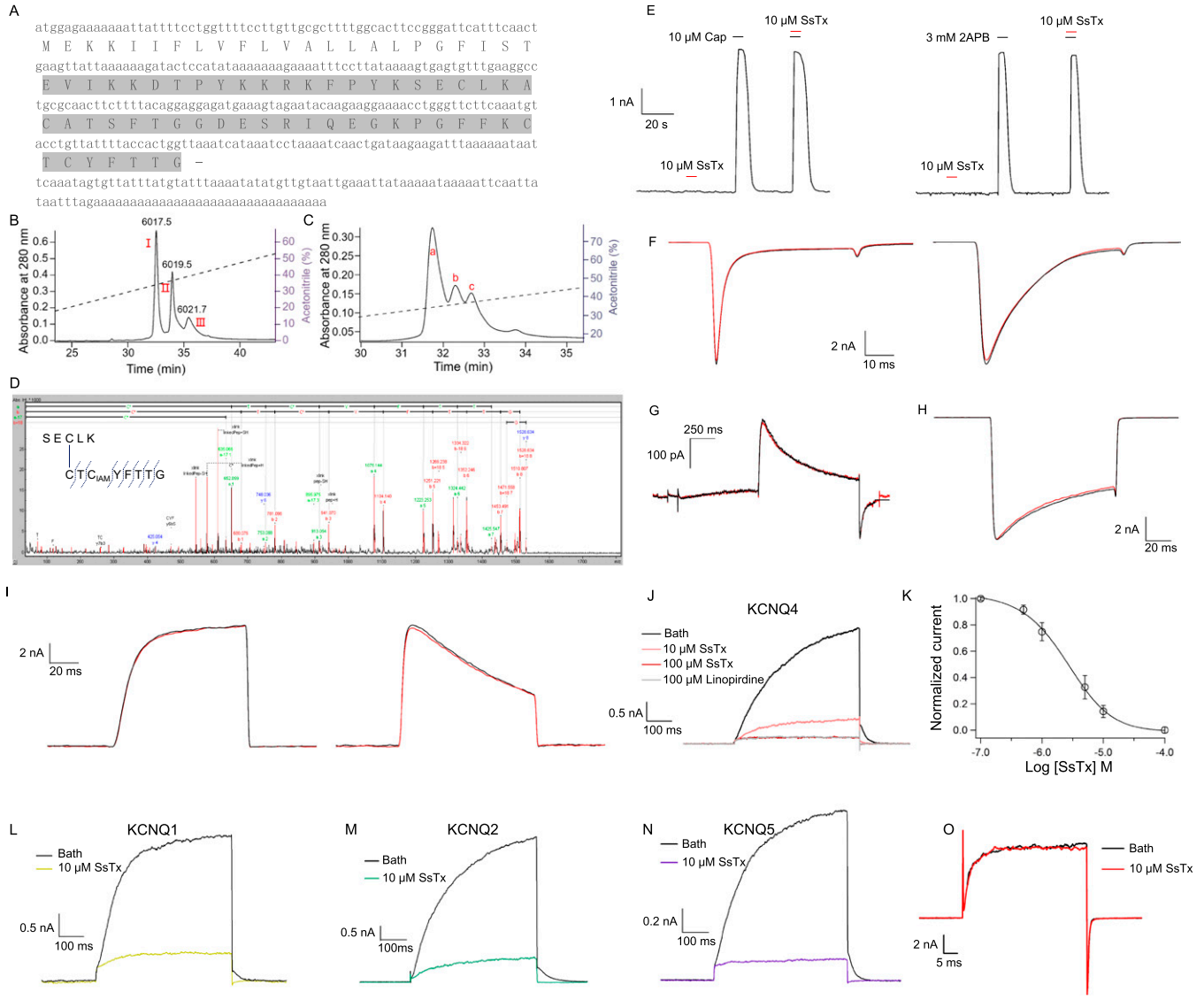

Fig. S1. SsTx is highly selective for KCNQ family. (*A*) The cDNA and amino acid sequences of SsTx, illustrating the signal and mature peptide (shaded). (*B*) Partial reduction of SsTx by TCEP fractionated by RP-HPLC. Three chromatographic peaks showed intact peptide (I), partially reduced intermediate (II), and completely reduced peptide (III). (*C*) Iodoacetamide alkylation of partially reduced SsTx purified by RP-HPLC. Three chromatographic peaks showing non-alkylated partially reduced SsTx (a) and alkylated one disulfide bond SsTx (b and c). (*D*) LIFT-TOF/TOF-MS analysis of enzymatic peptide by trypsin. A fragment with the mass of 1,528.6 Da was chosen to be analyzed as detailed in the *Inset* in which the solid line indicated the disulfide bridge pair determined. (*E–I*) The selectivity of 10 μM SsTx on TRPV1 channel (*E*, *Left*), TRPV2 channel (*E*, *Right*), TTX-sensitive sodium channels in DRG neuron (*F*, *Left*), TTX-resistant sodium channels in DRG neuron (*F*, *Right*), hERG channel (*G*), voltage-gated calcium channels in DRG neuron (*H*), Kv2.1 channel (*I*, *Left*) and Kv4.1 channel (*I*, *Right*). (*J*) Representative whole-cell KCNQ4 currents from the same HEK293T cell recorded in the presence of 10 μM SsTx, 100 μM SsTx, and saturated linopirdine (100 μM) sequentially. Before applications of each compound, the cells were perfused by bath solution for 30 s to ensure that the currents return to same level. (*K*) Dose–response relationships between SsTx and KCNQ4. The data were fitted to a Hill equation. The IC_{50} (average ± SEM) is 2.5 ± 0.4 μM (n = 10). (*L–N*) Representative whole-cell KCNQ1 (*L*), 2 (*M*), 5 (*N*) currents recorded in the presence and absence of 10 μM SsTx. (*O*) Representative whole-cell currents of mBK_{Ca} (mslo1) recorded in the presence and absence of 10 μM SsTx.

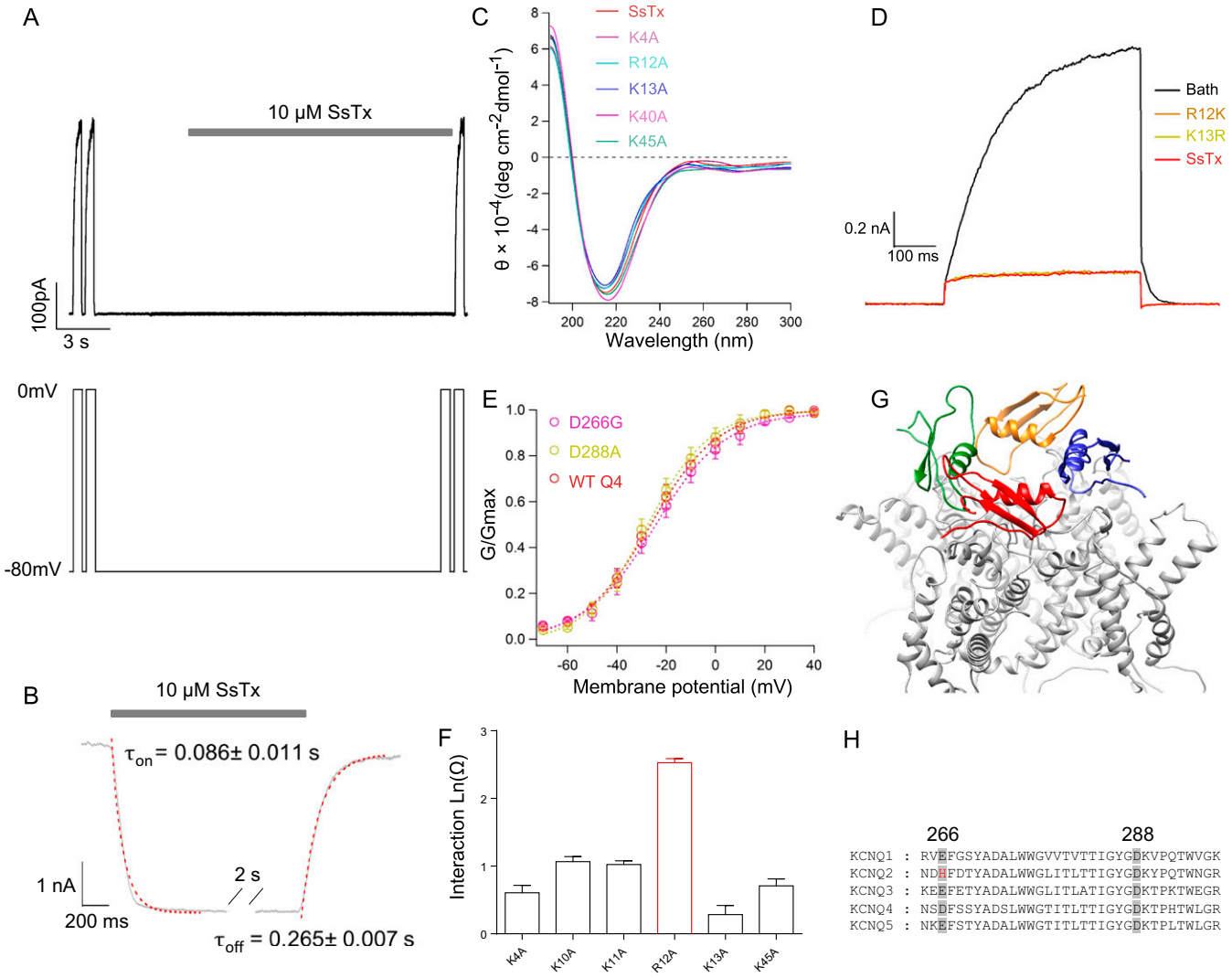

Fig. S2. WT or mutant SsTx interacted with WT or mutant KCNQ4 channels. (*A*) Representative whole-cell KCNQ4 currents in the presence and absence of 10 μM SsTx (*Top*) and the corresponding voltage protocol below (*Bottom*). (*B*) Representative time course of 10 μM SsTx-induced wash-in and wash-out recorded at 0 mV from a holding potential of −80 mV, superimposed with fittings of a single-exponential function (red dotted curves) and mean τ_{on} and τ_{off} values ($n = 3$ each). The speed of perfusion exchange was 5 ms. (*C*) CD spectra of WT and SsTx point mutants. (*D*) Representative whole-cell KCNQ4 currents in the presence of 10 μM WT, R12K, and K13R SsTx. The currents before the applications of each compound were washed by bath solution for 30 s. (*E*) Conductance–voltage relationships of WT KCNQ4, D266G, and D288A channel mutants. (*F*) Summary of interaction Ln(Ω) measurements for D288A channel mutant ($n = 3$–6 per bar). (*G*) The side view of docking model indicates multiple toxins target KCNQ4 channel. (*H*) Alignment of primary sequences of KCNQs from 264 to 297 (KCNQ4 number).

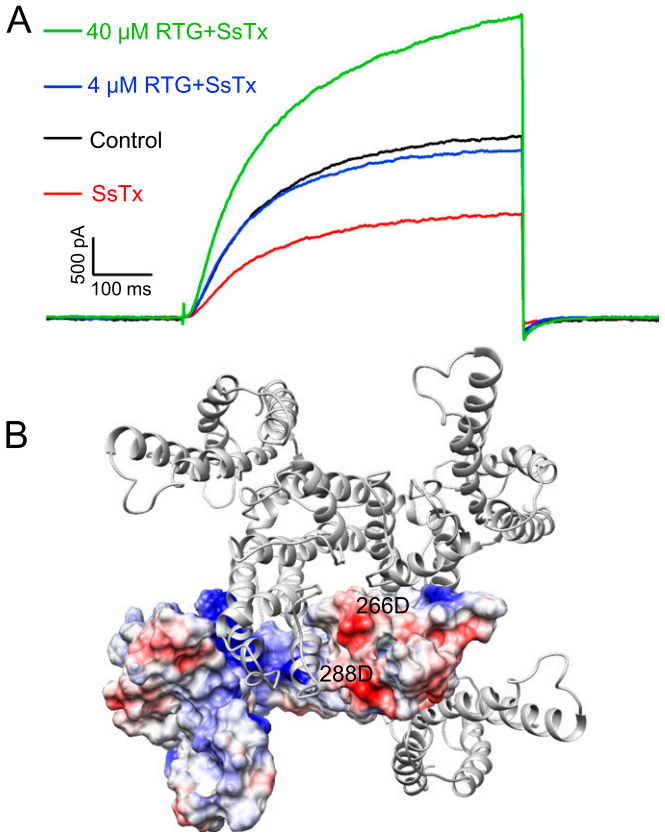

Fig. S3. RTG rescues SsTx-induced inhibition on KCNQ4 channel. (*A*) Representative whole-cell currents of KCNQ4 channel recorded from the same HEK293T cell. Before applications of each compound, the cells were perfused by bath solution for 30 s to ensure that the currents return to the same level. (*B*) Top view of KCNQ4 structural model with one subunit colored by surface electrostatic potential (red, negatively charged; blue, positively charged) and location of key residues (D266 and D288) identified by mutagenesis mapped to the KCNQ4 structural model. RTG, retigabine.

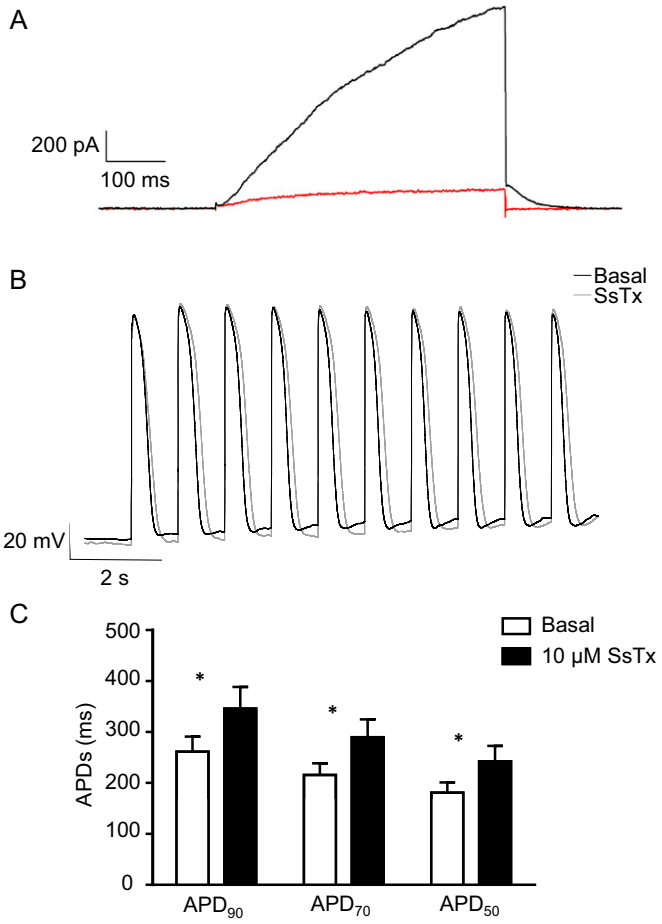

Fig. S4. Effects of SsTx on KCNQ1/KCNE1 complex and action potential of H9-CMs. (*A*) Representative whole-cell currents of KCNQ1/KCNE1 complex recorded in the presence (red) and absence (black) of 10 μM SsTx. (*B*) Representative action potential tracings recorded from H9-CMs by patch clamp before (black) and after (gray) treatment of 10 μM SsTx. (*C*) Bar graph comparison of APD_{90} (APD at 90% repolarization), APD_{70} (APD at 70% repolarization), and APD_{50} (APD at 50% repolarization) before (black) and after (gray) treatment of 10 μM SsTx. *$P < 0.05$ ($n = 3$ per bar). APD, action potential duration.

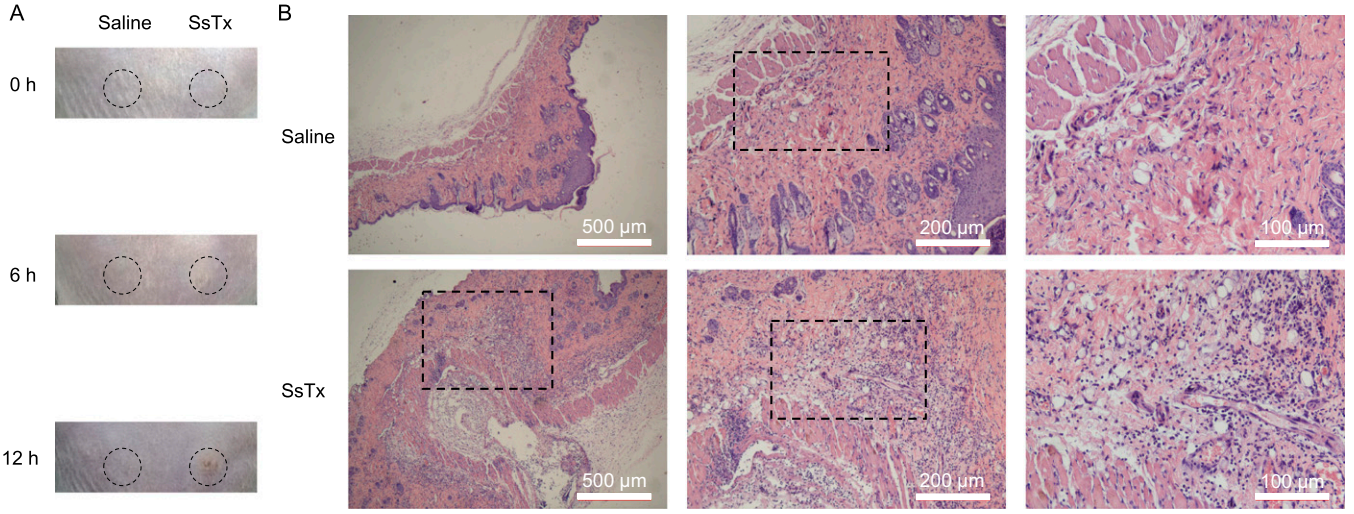

Fig. S5. SsTx induces tissue necrosis on mice. (*A*) Tracking the development of tissue necrosis phenotype on the back skin of mice between saline and SsTx. (*B*) The hematoxylin- and eosin-stained tissue sections analyzed by photomicrographs of the back skin taken from the same mouse.

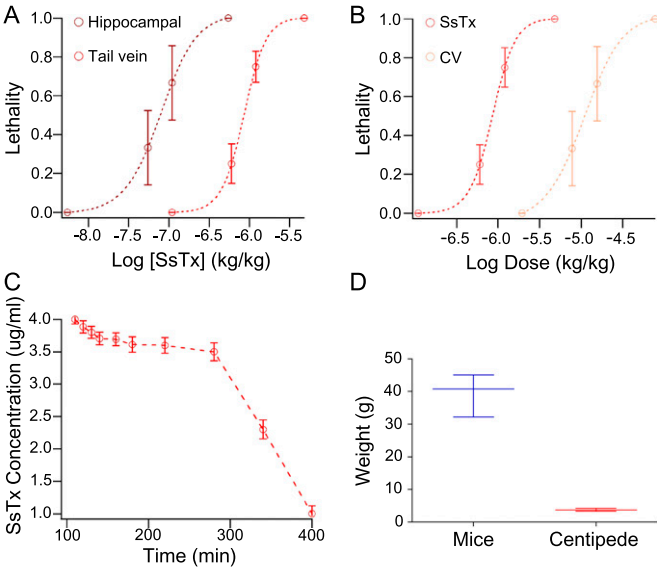

Fig. S6. Lethal toxicity of SsTx and CV. (*A*) Lethal dose of mice recorded after i.v. injection ($n = 4$ animals per group, $n = 3$ groups per point) and hippocampal microinjection ($n = 3$ animals per group, $n = 3$ groups per point) of SsTx and then fitted to a Hill equation. (*B*) The lethal dose of mice was recorded after i.v. injection of SsTx ($n = 4$ animals per group, $n = 3$ groups per point) and CV ($n = 3$ animals per group, $n = 3$ groups per point) and then fitted to a Hill equation. (*C*) Quantification of SsTx concentration in mouse plasma at varied durations by ELISA (tail vein; $n = 3$). (*D*) Statistical analysis of the weight of *S. subspinipes mutilans* ($n = 10$) and the Kunming mice ($n = 10$). CV, crude venom.

Movie S1. A single golden head centipede (*Scolopendra subspinipes mutilans*) weighing ~3 g attacks a mouse (~45 g) and rapidly subdues it within 30 s.

Movie S1

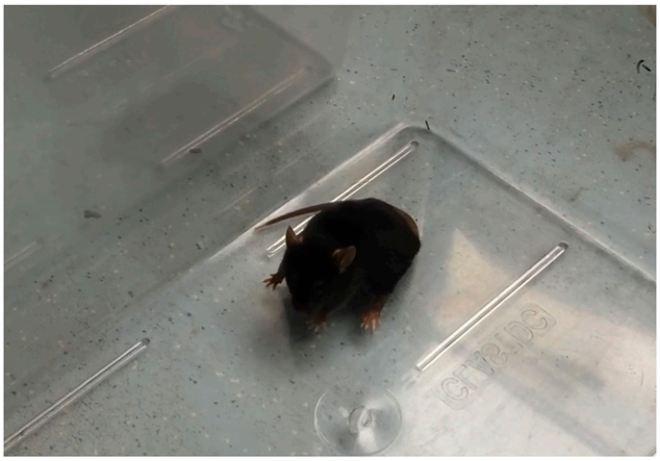

Movie S2. The mouse twitches and shakes before death following the i.v. injection of SsTx (4.79 mg/kg).

Movie S2

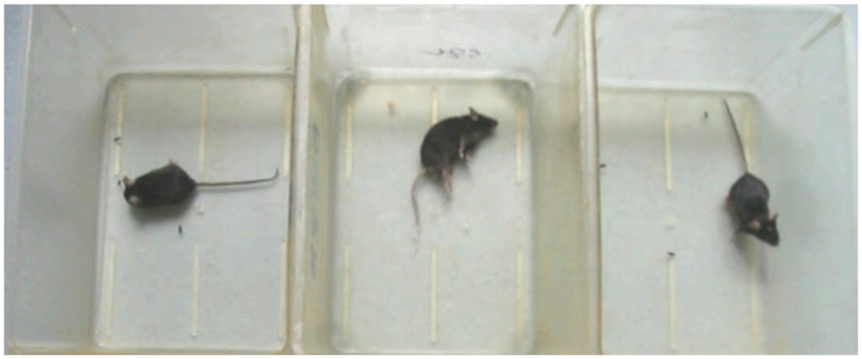

Movie S3. The behavior of mice after injection of 1 μL of 20 μM SsTx and 40 μM retigabine mixture (*Left*), 1 μL of 20 μM SsTx (*Middle*), and 1 μL saline (*Right*) in the hippocampus.

Movie S3